Interferometric measurement of the phase of diffracted waves near the plasmon resonances of metallic gratings

Nathalie Destouches, Hugues Giovannini, and Michel Lequime

We propose a method for analyzing both theoretically and experimentally the behavior of the phase of the waves diffracted by gratings. The method is applied to the study of resonance phenomena. It is used for determining the optogeometrical parameters of a metallic grating. We show that the experimental setup, which is insensitive to mechanical drifts or thermal fluctuations, can be used for sensing purposes. © 2001 Optical Society of America

OCIS codes: 050.1950, 260.3160.

1. Introduction

Electromagnetic resonances have been studied extensively, both theoretically and experimentally.[1,2] These phenomena, which can commonly be observed in optics, can have applications in various domains. For example, when a waveguide is placed in the vicinity of a prism illuminated in total reflection, under certain conditions the incident light can be coupled into the guide. This phenomenon has been used to detect bulk inhomogeneity in optical materials[3] or to determine the refractive index and the thickness of thin films for filtering applications.[4] Electromagnetic resonances can also be observed when the refractive index of a layer placed within a stack of thin films is spatially periodically modulated. If the stack is designed so that a propagation mode of the structure can be excited, then for a given angle of incidence a resonance can be obtained at a given wavelength.[5] In this case the guided mode is excited by the evanescent field generated by the grating. It has been shown that, in certain cases, the reflectivity can reach 100%.[5,6] Because the phenomenon is strongly sensitive to the wavelength, this technique is used to design narrow-band filters for telecommunication applications.[7] Resonance phenomena can also be observed by use of a metallic plane surface. In this case a prism is used to couple the incoming light into a surface wave whose amplitude decreases rapidly during propagation.[8] The resonance phenomenon leads to a strong variation of the structure's reflection coefficient. The amplitude of the diffracted light is strongly sensitive to the optogeometrical parameters of the structure and in particular to the refractive index of the region located in the vicinity of the metallic surface. Such sensitivity is used in commercial systems to detect low concentrations of species in chemistry or biology (see, for example, Refs. 9 and 10). The study of resonances on metallic plane surfaces can be extended to diffraction gratings. It has been shown that in certain conditions an incident plane wave can be totally absorbed by a shallow grating.[11] For a bare grating this phenomenon, which was first studied by Wood,[12] occurs only in TM polarization. The quick variation of the diffracted efficiencies (with respect to the incidence angle or to the wavelength) can be explained only by use of electromagnetic theory. Some studies have shown that the resonance is due to the existence of a pole in the diffracted efficiency.[13] As in the case of a plane surface, the resonance phenomenon can be used to study the presence of chemical reactions that occur near the grating's surface.[14]

Electromagnetic resonances of metallic gratings are usually detected by measurement of the variations of the diffracted efficiencies. However, it can be shown that the phases of the diffracted waves exhibit a particular behavior. In a previous paper

© 2001 Optical Society of America

Giovannini *et al.* measured such variations by means of an angle-resolved ellipsometer.[15] In the current paper, the variations of the phase of the diffracted waves relative to the angle of incidence are detected by means of an interferometric setup that has proved insensitive to thermal fluctuations or vibrations. The study of the phase both theoretically and experimentally allows us to determine the optogeometrical parameters of the grating. In certain cases we have found that the phase is more sensitive than the efficiency on the optogeometrical parameters of the grating. Some examples are presented to illustrate this property, which can be used to improve the sensitivity of systems used for sensing purposes.

In Section 2 we recall some well-known theoretical results on resonance phenomena. Section 3 provides an interferometric method to measure the phase of diffracted waves. In Section 4 we describe the experimental setup we developed to measure both the intensity and the phase of the diffracted orders of a metallic grating. In Section 5 we describe the configuration used for the measurements. In Section 6 we present the obtained results. These results were used, in Subsection 7.A, to determine, by use of a numerical code based on a rigorous method, the optogeometrical parameters (groove distance, height, refractive index of the metal, thickness and refractive index of a layer of oxide) of the grating. In Subsection 7.B we confirm that the phase can be calculated from a simple formula. In Section 8 we show that our principle of measurement can be used to improve the performances of sensing systems based on the detection of resonance phenomena.

2. Plasmon Resonances of Metallic Gratings

Wood[12] experimentally observed the anomalies of diffraction gratings in 1902. Since then we have been using the term Wood anomaly to describe every phenomenon that occurs when a slight modification of the characteristic parameters of the incident wave produces a strong variation of the grating efficiency. Among these singularities we take interest in those that result in a drop in the total diffracted efficiency when one of the diffracted orders propagates in the vicinity of the grazing direction. These phenomena can be observed with imperfectly conducting metallic gratings, in TM polarization (**H** parallel to the grooves). These singularities are commonly known as plasmon anomalies.[16]

From a mathematical point of view this kind of anomaly is a solution of Maxwell's equations with the associated boundary conditions, without any wave impinging on the structure. Researchers refer to such a solution as the resolution of a homogeneous problem[13]; the corresponding physical phenomenon is generally called a resonance. This phenomenon is attributed to the collective oscillations of electrons near the surface. The corresponding surface wave, which propagates along the periodic structure, carries energy parallel to the mean plane of the surface but is attenuated during propagation. Thus it is common to speak of leaky wave.

Let us consider a metallic grating illuminated at incidence angle θ. The wavelength-to-groove spacing ratio is chosen such that, in the incident medium, only the zero order propagates, with an amplitude B_0. The grating acts as a mirror, since the incident and the diffracted orders are symmetrical relative to the grating's normal. Thus the only interesting quantity from an experimental standpoint is B_0, which depends on $\alpha_0 = \sin \theta$. It also depends on the optogeometrical parameters of the grating, and it can be calculated by means of solving Maxwell's equations. Besides, in the case of periodic metallic surfaces, it has been shown[16] that $B_0(\alpha_0)$ can be approximated by a simple expression:

$$B_0(\alpha_0) \approx r(\alpha_0) \frac{\alpha_0 - \alpha^z}{\alpha_0 - \alpha^p}, \qquad (1)$$

where $r(\alpha_0)$ is the Fresnel reflection coefficient for a plane surface and α^Z and α^P are two complex numbers called zero and pole, respectively, which can be calculated numerically. It has been shown that the real parts of the pole and the zero of B_0 are close together.[11] Consequently the efficiency of the order exhibits a minimum value when $\sin \theta = \text{Re}\{\alpha^Z\} \approx \text{Re}\{\alpha^P\}$.

Assuming that $\alpha^Z = \alpha'^Z + i\alpha''^Z$ and $\alpha^P = \alpha'^P + i\alpha''^P$ with $\alpha'^Z \approx \alpha'^P$, the argument of B_0 can be written as follows:

$$\arg[B_0(\alpha_0)] = \arctan\left(\frac{-\alpha''^Z}{\alpha_0 - \alpha'^Z}\right) - \arctan\left(\frac{-\alpha''^P}{\alpha_0 - \alpha'^P}\right)$$
$$+ \arg[r(\alpha_0)]. \qquad (2)$$

The study of this function reveals a significant variation near $\alpha_0 = \alpha'^Z$. Thus the resonance phenomenon leads not only to a drop in the efficiency but also to a significant variation of the phase of the diffracted wave.

For dielectric coated gratings another type of resonance can be observed, with absorption weaker than for bare metallic gratings. When the layer is thick enough, the incoming wave can be coupled into a guided wave propagating within the layer. In this paper we are not concerned with this kind of resonance. In the more general case of a bare grating diffracting several radiative orders, the authors demonstrate that an element $S_{n,m}(\alpha_0)$ of the scattering matrix S defined by

$$\mathbf{B} = S\mathbf{A},$$

where **A** and **B** are vectors representing the normalized incident and the diffracted amplitudes, respectively, can be written as[13]

$$S_{n,m}(\alpha_0) = C_{n,m} \frac{\alpha_0 - \alpha_{n,m}{}^Z}{\alpha_0 - \alpha^P}, \qquad (3)$$

where $C_{n,m}$ is a complex number that depends on the optogeometrical parameters of the grating. Note that the pole is the same for all the orders.
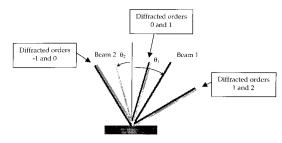
Fig. 1. Schematic representation of incident beams 1 and 2 and of the diffracted orders. θ_1 and θ_2 are the angles of incidence of beams 1 and 2, respectively.

3. Method of Measurement

In optics, measurements do not allow one to determine the phase of the diffracted waves directly. To solve this problem, we designed an experimental setup whose mainstay is an interferometer insensitive to mechanical drifts or thermal fluctuations. This section is devoted to the description of the method we used to measure both the efficiencies and the phase of the diffracted orders as a function of the incidence angle.

We consider the interference between two different orders propagating in the same direction, created by two coherent incident beams in TM polarization. The two beams illuminate the same area of the grating surface under two different incidence angles denoted θ_1 and θ_2 (see Fig. 1). These angles are chosen so that orders 0, 1, and 2 diffracted by the grating when illuminated by beam 1 will propagate in the same direction as orders -1, 0, and 1, respectively, created by beam 2 (Fig. 1). We denote $B_{n,m}$ the amplitude of the nth order created by the mth beam ($m \in \{1, 2\}$), with $\theta_{n,m}$ the angle between the grating's normal and the direction of propagation of the corresponding order, and $I_{n,m} = |B_{n,m}|^2$ the intensity. The light intensity that results from the coherent superposition of the two incident beams in the direction $\theta_{2,1} = \theta_{1,2}$ (channel a) is given by

$$I_a = |B_{2,1}(\alpha_0) + B_{1,2}(\alpha_0)|^2, \tag{4}$$

$$I_a = I_{2,1} + I_{1,2} + 2(I_{2,1}I_{1,2})^{1/2}\cos \psi_a, \tag{5}$$

where ψ_a is the phase shift defined by

$$\psi_a = \frac{2\pi\Delta}{\lambda} + \arg(B_{2,1}) - \arg(B_{1,2}). \tag{6}$$

The two interfering beams propagate from the beam splitter to the grating's surface. The optical path difference between them is Δ (see Fig. 2; from the surface to the detector, the optical paths of the two diffracted waves are identical). Equation (6) shows that ψ_a depends on Δ, which is sensitive to thermal fluctuations or mechanical drifts in the setup. This drawback can be eliminated if the grating diffracts at least three orders in the conditions of illumination, by use of a reference channel (measurement channel b). In this channel we observe another signal produced
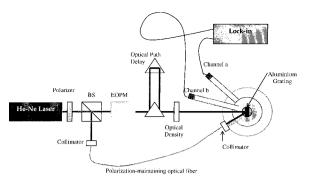

Fig. 2. Schematic of the experimental setup. The two detectors, the grating, and the optical fiber can be rotated independently around a vertical axis. The length of the optical path delay may be adjusted. The choice of an appropriate optical density allows one to maximize the amplitude modulation to continuous signal ratio. BS, beam splitter; EOPM, electro-optic lithium niobate phase operator.

by the interference between two other diffracted orders—each one produced by one of the incident beams. The analysis of the signals obtained in channels a and b permits us to calculate the phase difference

$$\begin{aligned}\psi(\theta_1) &= \pm[\psi_a(\theta_1, \theta_2) - \psi_b(\theta_1, \theta_2)] \\ &= \pm(\arg[B_{2,1}(\theta_1)] - \arg[B_{1,2}(\theta_2)] \\ &\quad - \{\arg[B_{1,1}(\theta_1)] - \arg[B_{0,2}(\theta_2)]\}) \end{aligned} \tag{7}$$

as a function of θ_1. Equation (7) shows that ψ is independent of Δ. The diffracted orders are superimposed; thus θ_1 and θ_2 are not independent. For this reason ψ can be considered to be a function of variable θ_1 only. Since the diffracted orders produced by the two incident beams are superimposed, when either incident beam is such that one of the diffracted orders propagates in a grazing direction, the same situation is obtained for the other. As a consequence, a plasmon resonance may occur for all the orders involved in the interference phenomenon.

4. Experimental Setup

The experimental setup we developed to measure the phase difference $\psi(\theta_1)$ is presented schematically in Fig. 2.

The He–Ne laser (wavelength $\lambda = 0.633$ μm) is TM polarized. The beam splitter (BS) produces two beams. Beam 1 propagates through an electro-optic lithium niobate phase modulator (EOPM). Beam 2 is coupled into a polarization-maintaining optical fiber. The collimated output beam illuminates the same area of the grating as beam 1.

The grating and the optical fiber can be rotated independently around a vertical axis. Thus both incidence angles θ_1 of beam 1 and θ_2 of beam 2 can be adjusted separately. Both beams are in the same plane of incidence. θ_1 and θ_2 are chosen so that the orders produced by the incident beams may be superimposed. The detectors are silicon photodiodes used in a photovoltaic mode. To observe the interference
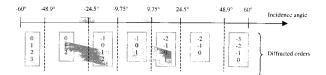
Fig. 3. Diffracted orders for different values of the angle of incidence. Grating period $d = 1.082$ μm and wavelength $\lambda = 0.633$ μm. Shaded areas correspond to the variation range of i_1 and i_2 around a resonance. Measurements are made on the highlighted orders.

Fig. 5. Measured phase difference ψ as a function of θ_1.

phenomena for all incidence angles θ_1 and θ_2, the detectors are mounted on separate arms that can rotate around a vertical axis.

By applying a sawtooth voltage modulation on the EOPM, whose amplitude corresponds to a 2π phase shift at operating wavelength, we induce a linear phase modulation in beam 1. This allows us to obtain a pure cosine electrical signal in each channel, whose frequency is equal to that of the sawtooth signal. By using a lock-in amplifier in its phase detection mode, we measure the phase term ψ of Eq. (7).

The use of an adjustable optical-path-delay assembly allows rough equalization of the optical path of the two arms of the interferometer, which prevents a possible decrease in the visibility of the interference phenomena induced by the relatively small coherence length of the source ($\sim$10 cm). Using an optical density, we can adjust the intensity of the two beams in order to increase modulation amplitude to continuous signal ratio. The optical density is chosen so that maximum visibility of the interference phenomenon is obtained in channel b, i.e., the reference channel of the lock-in amplifier.

5. Measurement

A holographic aluminum grating with 924 grooves/mm (grating period $d = 1.082$ μm) was studied by use of the system described in Section 4. In normal incidence the grating diffracts three orders at
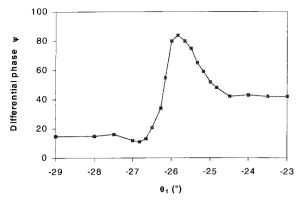
$\lambda = 0.633$ μm. The grating formula applied with $\theta_{n,1} = \pm 90°$ allows us to calculate the incidence angle θ_{1L} for which the nth order becomes radiative,

$$\theta_{1L} = \arcsin\left(\pm 1 - n\,\frac{\lambda}{d}\right). \qquad (8)$$

Figure 3 shows the number of diffracted orders as a function of the incidence angle. Because the diffracted orders created by the two incident beams are superimposed, θ_1 and θ_2 must verify

$$\sin\theta_2 = \sin\theta_1 + k\,\frac{\lambda}{d}, \qquad (9)$$

where k is an integer. Because of the grating period and the operating wavelength, k can be equal either to +1 or to -1. The range of variation of θ_1 has been chosen to

- excite a resonance,
- avoid problems that are due to the obstruction of the beams by mechanical parts,
- work at low-incidence angles to limit the size of the illuminated surface of the grating.
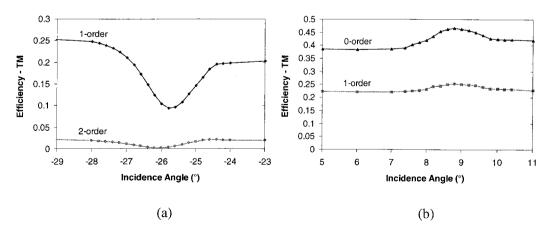

(a)

(b)

Fig. 4. Measured efficiencies of the orders involved in the determination of differential phase ψ. The measurements are made in the vicinity of two resonances. Incidence angles θ_1 and θ_2 are linked by Eq. (9). (a) Efficiencies of diffracted orders 1 and 2 as a function of θ_1 (incident beam 1). (b) Efficiencies of diffracted orders 0 and 1 as a function of θ_2 (incident beam 2).
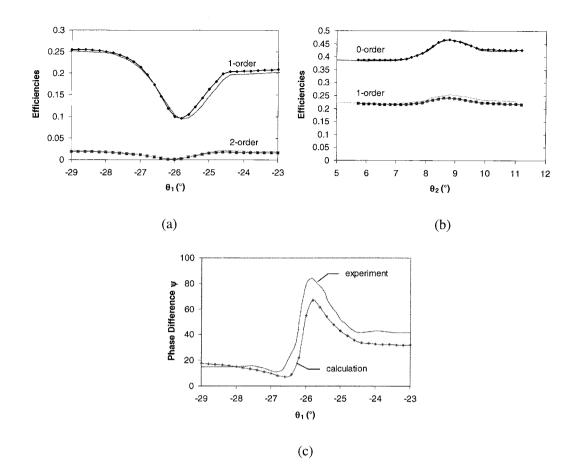
Fig. 6. Comparison between experimental results (plain solid curve) and numerical results (marked curve). (a) Efficiencies of orders 1 and 2 as a function of θ_1 (incident beam 1). (b) Efficiencies of orders 0 and 1 as a function of θ_2 (incident beam 2). (c) Phase difference ψ as a function of θ_1.

These considerations led to the choice of $k = 1$. Consequently, if θ_1 varies in the interval $[\theta_1^{\min}; \theta_1^{\max}]$, then θ_2 varies in the interval

$$\left[\arcsin\left(\sin\theta_1^{\min} + \frac{\lambda}{d} \right); \arcsin\left(\sin\theta_1^{\max} + \frac{\lambda}{d} \right) \right].$$

θ_1 was chosen to vary within the interval $[-29°; -23°]$ and θ_2 within the interval $[5.73°; 11.18°]$ (see Fig. 3).

6. Experimental Results

The sample is a holographic aluminum-coated sinusoidal grating. The grating period $d = 1.082$ μm was determined by use of a Littrow mount. We measured the efficiencies, in TM polarization, of four diffracted

orders as a function of the incidence angle by using the experimental setup described in Fig. 2. As predicted by theory, the efficiency of the $+1$ order was found to be symmetric to that of the -1 order with respect to $\theta_1 = 0$. In addition, we noted that the efficiency in the -1 order for an incidence angle θ_1 varying near the resonance is identical to the efficiency in the $+1$ order for an incidence angle θ_1' so that $\sin\theta_1 - k(\lambda/d) = \sin\theta_1'$. This can be written by use of the notation in Section 3 in the form $I_{-1,2} = I_{1,1}$.

Figure 4 shows the experimental results obtained when the grating is illuminated in the vicinity of the resonance.

Phase ψ was measured relative to the angle of in-

Table 1. Values of the Complex Pole and Zero and of the Square Modulus of Constant C for Each Order Involved in the Calculation of Differential Phase ψ^a

	Order 1, Beam 1	Order 2, Beam 1	Order 0, Beam 2	Order 1, Beam 2
$\lvert C \rvert^2$	2.553×10^{-1}	2.6929×10^{-2}	3.8762×10^{-1}	2.2219×10^{-1}
α'^Z	-4.3546×10^{-1}	-4.3928×10^{-1}	1.48556×10^{-1}	1.48781×10^{-1}
α''^Z	9.807×10^{-3}	4.543×10^{-3}	1.6238×10^{-2}	1.5796×10^{-2}
α'^P	-4.37032×10^{-1}	-4.37032×10^{-1}	1.4929×10^{-1}	1.4929×10^{-1}
α''^Z	-1.5831×10^{-2}	-1.5831×10^{-2}	1.4889×10^{-2}	1.4889×10^{-2}

^{a}We determined the values by fitting efficiency curves, by using Eq. (3).
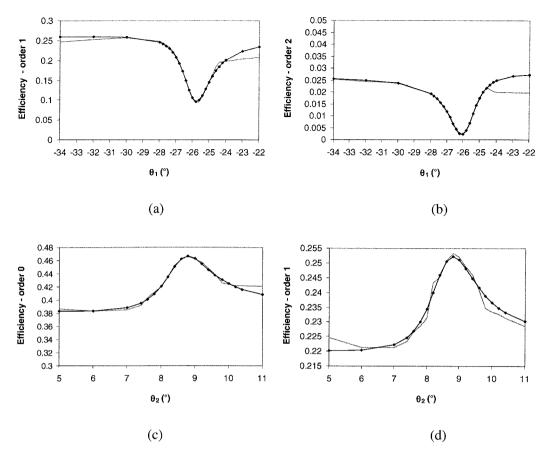
(a)

(b)

(c)

(d)

Fig. 7. Comparison between experimental results (plain solid curve) and numerical results (marked curve) in the vicinity of the resonance. The efficiencies are calculated from Eq. (3). For the calculation the values of the parameters of Table 1 have been taken. (a) Efficiency of order 1 produced by beam 1 as a function of θ_1 (incident beam 1). (b) Efficiency of order 2 as a function of θ_1 (incident beam 1). (c) Efficiency of order 0 produced by beam 2 as a function of θ_2 (incident beam 2). (d) Efficiency of order 1 produced by beam 2 as a function of θ_2 (incident beam 2).

cidence. When the sawtooth signal applied to the electro-optic phase modulator is used as the reference signal of the lock-in amplifier, the phase measurement becomes extremely sensitive to the instabilities of the setup. This effect clearly brings out the advantage of the configuration described in Fig. 2. ψ
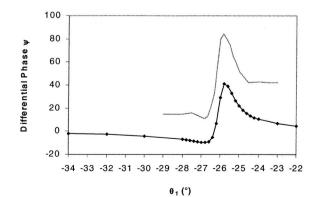

Fig. 8. Comparison between measured phase ψ (plain solid curve) and phase ψ calculated from Eqs. (2) and (7) (marked curve). For the calculation the values of the parameters of Table 1 have been taken.

was measured with an accuracy better than 1° for a bandpass of 1 Hz. The result of the phase measurement is shown in Fig. 5. We can observe a strong variation of the phase ψ near the plasmon resonance.

The repeatability of the measurement has proved be better than 1% in the measurement span.

The experimental results were used to determine the optogeometrical parameters of the grating. The refractive index of aluminum, the thickness of the oxide layer, and the groove's height were determined with approximately 5% accuracy by fitting of the experimental curves to the curves given by a numerical simulation.

7. Numerical Calculations

A. Resolution of Maxwell's Equations

Calculations were made with a computer code based on the differential formalism[17] with the S-matrix algorithm.[18,19] The code gives the efficiency and the phase for each diffracted order. Both the curves giving the efficiencies and those giving the phase ψ were taken into account. A plane area on the aluminum-covered substrate allowed us to determine the reflection coefficient R of the metallic surface. A value of
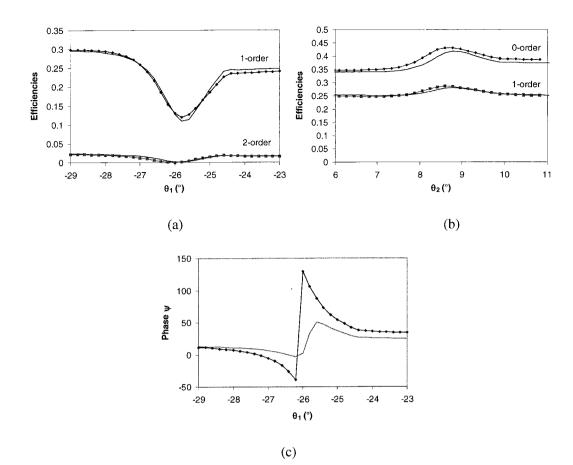
Fig. 9. Sensitivity to the thickness of the region located near the grating's surface. Numerical results obtained for $h = 0.11$ μm, $\nu = 1.23 + i9.6$, $\nu_{ox} = 1.63$, 924 grooves/mm, and $h_{ox} = 13$ nm (plain solid curve) or $h_{ox} = 15$ nm (marked curve). (a) Efficiencies of orders 1 and 2 as a function of θ_1 (incident beam 1). (b) Efficiencies of orders 0 and 1 as a function of θ_2 (incident beam 2). (c) Differential phase ψ as a function of θ_1.

$R = 0.9$ was found at $\lambda = 0.633$ μm. Knowing this quantity allowed us to link the real part n and the imaginary part k of ν ($\nu = n + ik$, with $i^2 = -1$) as given by Eq. (10):

$$k = \left(-n^2 - 1 + 2n\,\frac{1+R}{1-R} \right)^{1/2}. \qquad (10)$$

To obtain good agreement between experimental results and numerical ones, we had to consider a thin layer of alumina (Al$_2$O$_3$) of thickness $h_{ox} = 12$ nm and with a refractive index $\nu_{ox} = 1.63$. Figure 6 shows the results obtained with grating depth $h = 0.102$ μm, and the refractive index of aluminium $\nu = 1.5 + i7.33$. Good agreement is found between numerical results and experimental ones. The small discrepancies obtained for the phase curves can be attributed to scattering effects produced by the roughness of grating's surface. The values found for the grating's depth and for the period were confirmed by atomic force microscopy measurements showing that approximately 3% accuracy was obtained.

B. Research for the Poles and Zeros at the Resonance

Assuming that the efficiency of the diffracted orders can be calculated from Eq. (3) in the vicinity of the

resonance, we searched for the zeros, the poles, and the square modulus of complex constants $C_{n,m}$ (see Table 1) for the orders involved in the measurement, by fitting the experimental curves. Note that all the orders produced by the same incident beam have the same pole. Moreover, the real part of a pole is close to the real part of the corresponding zero. These conclusions are in agreement with previous publications.[16] Away from the resonance, Eq. (3) cannot be used. The difference between experimental and numerical results observed at $\theta_1 = -24.5°$ and $\theta_2 = 9.8°$, respectively, is due to the apparition of orders -1 and order -2, respectively (see Fig. 3). The obtained values allowed us to calculate the differential phase ψ from Eqs. (7) and (2) analytically.

Figure 7 permits one to compare the efficiencies calculated from Eq. (3), by use of the values of the parameters of Table 1, with those experimentally obtained. One can observe that strong agreement is found near the resonance.

The results shown in Fig. 8 concern phase ψ. Except for the offset value of the curve numerically obtained, good agreement is found between theoretical results and experimental ones. A fit on the efficiency curves allows one to determine only $|C_{n,m}|^2$.

Then the arguments of complex constants $C_{n,m}$ are undetermined. This problem explains the offset of the numerical curve of Fig. 9, which is equal to $\pm[\arg(C_{2,1}) - \arg(C_{1,2}) - \arg(C_{1,1}) + \arg(C_{0,2})]$. The results of Fig. 9 confirm the validity of Eq. (3) for describing the amplitude of the diffracted field near the resonance.

8. Advantages of the Method

The main advantage of the measurement method described in this paper is that it does not require either precise alignments or mechanical or thermal stabilization. Another advantage is that the sensitivity of the phase to the external parameters (refractive index of a region located near the grating's surface, for example) can be increased in the vicinity of a resonance. Indeed it is possible to determine a configuration for which the phase variations of the two orders that interfere in channel a have opposite signs. In this case the variation of differential phase ψ would be stronger than that of the phase of each order. This effect, which cannot be obtained with a polarimetric configuration, can be useful for sensing applications. Moreover, phase measurements provide useful information about diffracting structures. Figure 9 shows that a small variation of the thickness of the oxide layer induces only a slight variation of the diffracted efficiency. Yet the variation of the thickness causes the phase to vary strongly.

9. Conclusion

We have demonstrated the operating principle of an interferometer designed to measure the phase difference between two orders diffracted by a grating, as a function of the incidence angle. The measurement method has been applied to study electromagnetic resonances and used to determine the optogeometrical parameters of a metallic grating. A theoretical study of the phase variation around the resonance has been carried out, and good agreement has been found between numerical results and experimental ones. We have shown that the interferometric setup described in this paper can be used for sensing purposes. The possibility of obtaining information about the phase of the diffracted wave opens the way for the study of inverse problems in optics.

References

1. R. C. McPhedran and D. Maystre, "A detailed theoretical study of the anomalies of a sinusoidal diffraction grating," Opt. Acta **21,** 413–421 (1974).
2. M. C. Hutley and D. Maystre, "The total absorption of light by a diffraction grating," Opt. Commun. **19,** 431–436 (1976).
3. C. Amra and S. Maure, "Mutual coherence and conical pattern of sources optimally excited within multilayer optics," J. Opt. Soc. Am. A **14,** 3114–3124 (1997).
4. F. Flory, "Guided wave techniques for the characterization of optical coatings," in *Thin Films for Optical Systems*, F. Flory, ed., Vol. 49 of Optical Engineering Series (Marcel Dekker, New York, 1995), pp. 393–454.
5. P. Vincent and M. Nevière, "Corrugated dielectric waveguides: a numerical study of the second-order stop bands," Appl. Phys. **20,** 345–351 (1979).
6. G. A. Golubenko, A. S. Svakhin, V. A. Sychugov, and A. V. Tischenko, "Total reflection of light from a corrugated surface of a dielectric waveguide," Sov. J. Quant. Electron. **15,** 886–887 (1985).
7. R. Magnusson and S. S. Wang, "New principle for optical filters," Appl. Phys. Lett. **61,** 1022–1024 (1992).
8. V. Shah and T. Tamir, "Brewster phenomena in lossy structures," Opt. Commun. **23,** 113–117 (1977).
9. K. Matsubara, S. Kawata, and S. Minami, "Optical chemical sensor based on surface plasmon measurement," Appl. Opt. **27,** 1160–1163 (1988).
10. M. Zhang and D. Uttamchandani, "Optical chemical sensing employing surface plasmon resonance," Electron. Lett. **24,** 1469–1470 (1988).
11. D. Maystre, "General study of grating anomalies from electromagnetic surface modes," in *Electromagnetic Surface Modes*, A. D. Boardman, ed. (Wiley, New York, 1982), pp. 661–724.
12. R. W. Wood, "On a remarkable case of uneven distribution of light in a diffraction grating spectrum," Phil. Mag. **4,** 396–408 (1902).
13. M. Nevière, "The homogeneous problem," in *Topics in Current Physics, Electromagnetic Theory of Gratings*, R. Petit, ed. (Springer-Verlag, Berlin, 1980), pp. 123–157.
14. M. J. Jory, P. S. Vukusic, and J. R. Sambles, "Development of a prototype gas sensor using surface plasmon resonance on gratings," Sens. Actuators B **17,** 203–209 (1994).
15. H. Giovannini, C. Deumié, H. Akhouayri, and C. Amra, "Angle-resolved polarimetric phase measurement for the characterization of gratings," Opt. Lett. **21,** 1619–1621 (1996).
16. D. Maystre and M. Nevière, "Sur une méthode d'étude théorique quantitative des anomalies de Wood des réseaux de diffraction: application aux anomalies de plasmon," J. Opt. (Paris) **8,** 165–174 (1977).
17. P. Vincent, "Differential methods," in *Progress in Optics*, E. Wolf, ed. (Springer-Verlag, Berlin, 1980), Vol. 22, pp. 101–121.
18. F. Montiel and M. Nevière, "Differential theory of gratings: extension to deep gratings of arbitrary profile and permittivity through the R-matrix algorithm," J. Opt. Soc. Am. A **11,** 3241–3250 (1994).
19. L. Li, "Formulation and comparison of two recursive matrix algorithms for modeling layered diffraction gratings," J. Opt. Soc. Am. A **13,** 1024–1035 (1996).